Carbon Science

Vol. 1, No. 1 June 2000 pp. 6-11

Activated Carbon Fibers from Chemically Modified Coal Tar Pitches

S. K. Ryu[1,*], J. W. Shim[1], K. S. Yang[2] and I. Mochida[3]

[1]Dept. of Chemical Engineering, Chungnam National University, Taejon 305-764, Korea
[2]Dept. of Textile Engineering, Chonnam National University, Kwangju 500-757, Korea
[3]Institute of Advanced Materials Study, Kyushu University, Fukuoka 816, Japan
*e-mail: *skryu@cuvic.chungnam.ac.kr*

(Received 14 February 2000; accepted 26 May 2000)

Abstract

Coal tar pitch was chemically modified with 10 wt% benzoquinone (BQ) to raise the softening point of isotropic pitch precursor and the precursor was melt-spun into pitch fibers, stabilized, carbonized and activated with steam at 900°C. The weight loss of carbon fiber-benzoquinone (CF-BQ) increased with the increase of activation time like other fibers, but was lower than those of Kureha fiber at the same activation time in spite of larger geometric surface area. Those adsorption isotherms fitted into 'Type I' according to Brunauer, Deming, Deming and Teller classification. However, there was very thin low-pressure hysteresis that lower closure points of the hysteresis are about 0.42-0.45. From the pore size distribution curves, there might be some micropores having narrow-necked bottle; a series of interconnected pore is more likely than discrete bottles. FT-IR studies showed that the functional groups such as carboxyl, quinone, and phenol were introduced to ACFs-BQ surface after steam activation. Methylene blue decolorization and iodine adsorption capacity of ACF-BQ increased linearly with the increase of specific surface area and was larger than that of ACF-Kureha at the same specific surface area.

Keywords : *ACF, Coal tar pitch, BET surface area, Functional groups*

1. Introduction

Recently, much attention has been focused on activated carbon fibers (ACFs). ACF has a remarkably rapid rate of adsorption for solvent recovery, deodorization and the removal of contaminants from water and gases. The application of ACF is extended not only adsorbents but also catalyst supports, electrical and electronic materials for its unique pore structure and sufficient level of electrical conductivity. Thus efforts have been under way to prepare cheaper ACFs with controlled pore size distribution, high surface area and designed functional groups. ACFs have been manufactured from rayon, polyacrylonitrile, phenolic-resin, and pitches in a two-step process of carbonization of the raw material and successful activation. Among the ACFs, pitch-based one appears most promising in the future because of low cost and unique properties.

Spinnability of pitch is depended on its chemical composition and molecular weight distribution [1]. Although any spinnable pitch with high carbon yield can be used as a precursor of general purpose carbon fiber in principle, a qualified precursor must satisfy the following two requirements. Firstly, higher softening point is preferable as far as stable spinning is assured, since stabilization at higher temperature is allowed for such a pitch precursor to complete its stabilization in a short period of time. Secondly, the pitch must be completely isotropic, because contamination by any mesophase spheres of which the viscosity-temperature relationship is very different from that of the isotropic part severely deteriorates the spinnability of the whole pitch.

Air blowing has been successfully applied in preparing precursors for isotropic carbon materials and in raising the softening point of coal tar or petroleum feed stocks [2]. Mochida et al. [3] obtained coal tar pitch precursor with softening point of 280°C by air blowing. However, the air blowing requires severe control of conditions in blowing time and temperature. Yang et al. [4] reported that coal tar pitch was polymerized with benzoquinone (BQ) at about 150°C resulting in an increase in molecular size without development of anisotropy.

In this study, coal tar pitch chemically modified with 10 wt% BQ was examined as a precursor to produce ACF through spinning, stabilizing, carbonizing, and activating. The advantage of the high yield after the carbonization as well as activation was most concerned. Porosity in the ACF was also measured to understand its characteristics.

2. Experiment

Tetrahydrofuran (THF) soluble fraction of the coal tar pitch (s.p. 85°C, Jung-Woo Coal Chem. Co., Korea) was oligomerized with 10 wt% *p*-benzoquinone (BQ) under nitrogen flow at 131°C for 1 h, and further heat treated with nitrogen bubbling at 380°C for 3h. The softening point of the chemically modified isotropic pitch was 271°C and the other properties were introduced in a previous report [5]. This precursor pitch was aged for 3h at 330°C under nitrogen flow and then melt-spun through a nozzle (D = 0.3 mm, L = 0.6 mm) at 285°C, 10 kg_f/m^2. The spinning speed was 480 m/

min. The as-spun fiber was stabilized in an air convection oven at 330°C for 3h. The fiber was carbonized at 1000°C with heating rate of 5°C/min and held for 1h under argon flow. This isotropic pitch-based carbon fiber is named CF-BQ. The average fiber diameter was 17 μm.

The CF-BQ was activated by steam diluted with nitrogen in a cylindrical quartz tube (I.D = 5 cm) installed in an electric furnace at different levels of burn-off at 900°C. The nitrogen flow rate and volume ratio of H_2O/N_2 were fixed at 1.6 l/min and 0.44, respectively in all cases. The extent of activation is expressed in % of weight loss after gasification. The Kureha isotropic pitch-based carbon fiber (KCF-100, average diameter 14 μm) was also activated for comparison. Thus prepared ACFs were named ACF-BQ and Kureha. Percentage attached described the extent of burn-off.

Specific surface areas of ACFs were determined by BET method using N_2 at 77 K. The microporous volume and the external surface area were determined by using α_s-method [6]. The samples were degassed at 470 K under dynamic vacuum (10^{-4} Pa) for 15h and an adsorption time of 30 min was allowed for each point (ASAP 2400, Micromeritics, U.S.A.). The surface morphologies of different level of ACFs were observed with SEM (JSM 5400, Japan). The surface functional groups of the ACFs-BQ were analyzed by FT-IR spectrophotometer using Genesis 2000 series (Mattson Co., U.S.A) [7]. Adsorption tests of iodine and methylene blue from aqueous solution were carried out following the conventional method [8].

3. Results and Discussion

3.1. Structural properties

The weight loss of carbon fiber with respect to activation time was shown in Fig. 1. The dotted line is the result of activation of Kureha isotropic pitch-based carbon fiber (KCF-100) for comparison with CF-BQ. The weight loss increased with the increase of activation time like other fibers. However, the weight loss of CF-BQ was smaller than that of general isotropic pitch-based carbon fibers [9] and of Kureha fiber at the same activation time in spite of larger geometric surface. This means the CF-BQ is thermally more stable than Kureha fiber. It is believed that the CF-BQ has different orientation structure from other fibers because of oligomeration of precursor pitch. If the specific surface area or the total pore volume of ACF-BQ-40% was same to that of ACF-Kureha-40%, ACF-BQ would need longer activation time, which means 33% higher energy consumption than ACF-Kureha. On the other hand, the yield of ACF-BQ is about 25% higher than that of ACF-Kureha at the same activation time. Therefore, in determining the optimum activation condition of ACF, it can be assumed that the adsorption characteristics and capacities are more important than any other factors.

The adsorption isotherm of ACFs-BQ-76% was shown in Fig. 2. The isotherm shows 'Type I' with sharp knee and then plateau as other ACFs-BQ. This means there are enormous micropores in the fibers. The amount of nitrogen adsorption increased remarkably with the increase of burn-off level. There are very thin 'low-pressure hysteresis' on all isotherms, which could not be observed from the ACF-Kureha and other isotropic pitch-based ACFs. The precursor pitch modified with benzoquinone surely affected the characteristics of carbon fibers and activated carbon fibers. The lower closure points of the hysteresis are about 0.42-0.45. Harris [10] draw attention from the fact that the low closure point of the hysteresis loop of nitrogen isotherm at 77 K is situated at the relative pressure close to 0.42 but never below: one-half of more than one hundred nitrogen isotherms in the literature examined by Harris shows a sharp fall, with loop closure, in the relative pressure range of 0.42 to 0.50. Interpreted by a Kelvin type analysis, these observations would imply that a large proportion of adsorbents pos-

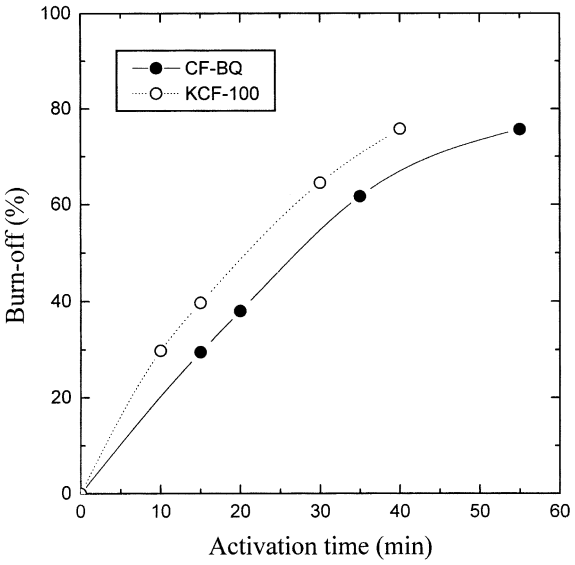

Fig. 1. Weight loss of CF-BQ with respect to activation time at 900°C.

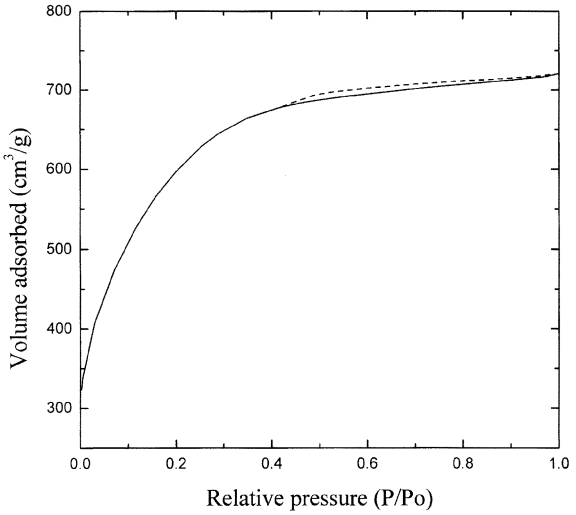

Fig. 2. Adsorption isotherms of ACFs-BQ: (a) 30%, (b) 38%, (c) 62%, (d) 76% weight loss.

Table 1. Nitrogen Adsorption Characteristics of ACFs-BQ

Burn-off (%)	S_{BET} (m^2/g)	Average pore Dia. (Å)	Total pore Vol. (cm^3/g)	Micropore Vol. (cm^3/g)	S_{ext} (m^2/g)
0	207	17.3	0.089	0.08	0.8
30	954	18.6	0.44	0.43	3.6
38	973	20.0	0.49	0.48	5
62	1830	19.8	0.91	0.89	8
76	2131	20.9	1.11	1.08	17

sess an extensive pore system in the very narrow range 17Å < r^p < 20Å, with a sudden cut-off around 17Å, which corresponds to P/P^o = 0.42. The improbability of this state of affairs led Harris to suggest that a change in the mechanism of adsorption occurred at this point, though he did not speculate as to its nature. The similar results have reported by several researchers [11, 12]. Tayyab [13] reported that the position of the closure point was almost the same at ~0.42 with a mesoporous magnesia.

Gas adsorption characteristics of some ACF-BQ were shown in Table 1. The unactivated carbon fiber (CF-BQ) possesses about 207 m^2/g of specific surface area that is quite different from other isotropic pitch-based carbon fibers. In general, the other unactivated carbon fibers possess the surface area close to its geometric surface area (0.2 m^2/g). In addition, the average pore diameter of CF-BQ is 17.3Å which is far larger than those of other carbon fibers. Also, the micropore volume of unactivated carbon fiber is almost same to the total pore volume, and the external surface area is very small. This means that there are already lots of micropores in the fibers which contribute to increase specific surface area. These micropores must have developed during the carbonization of pitch fibers.

The specific surface area and the total pore volume of ACF-BQ increased with the increase of burn-off. The micropore volume is close to the total pore volume, which is showing that the newly developed pores are almost micropores. This is confirmed by the small increase of external surface area with respect to burn-off. The average pore diameter of ACF-BQ increases from 17.3Å to 18.6Å at 30% burn-off and then shows interestingly constant values about 20Å with the increase of burn-off, which is twice as large as those of general purpose isotropic ACFs [14]. In general, the average pore diameter of isotropic-pitch based ACF is about 10Å and slightly enlarged as the burn-off increase. How can we explain the development of larger micropore diameter of ACFs-BQ in spite of thermally more stable than Kureha carbon fibers. Probably, benzoquinone may have contributed to enhance the orientation of isotropic pitch fiber along the axial direction of fiber. Therefore, most micropores developed might have slit shapes of narrow range along the fiber direction. The lower closure point of the hysteresis loop in Fig. 2 has already indicated that there are only the narrow range of pores in ACFs-BQ.

The relationship between burn-off and specific surface area was shown in Fig. 3. The specific surface area increased

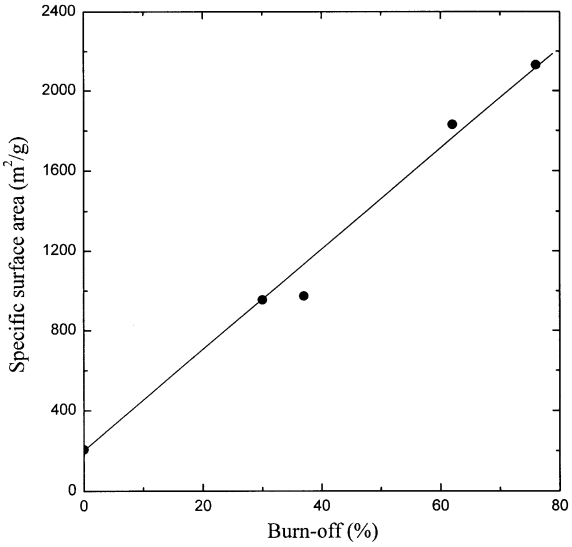

Fig. 3. Specific surface area of ACFs-BQ with respect to weight loss at 900°C.

linearly with the increase of burn-off as expected. Interestingly, the specific surface area of ACF-BQ is far larger than that of other pitch-based ACFs at the same level of burn-off [9]. It is believed that there is not only a little external weight loss but also much internal weight loss of CF-BQ with increasing the burn-off in comparison with other pitch-based carbon fibers.

Fig. 4 shows the pore size distribution of ACFs-BQ determined by adsorption of nitrogen at 77 K. Each curve indicates that the amount of pore volume increase and the pore size are gradually changed from narrow range to wide range according as the weight loss of ACF-BQ increase like Table 1. On the other hand, a new peak was developed distinctly around 14Å pore width. In the curve of ACF-BQ at 76% burn-off level, a peak was divided into two parts clearly.

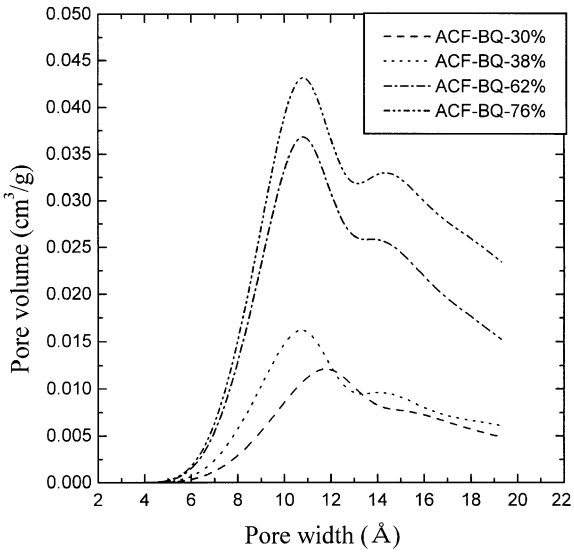

Fig. 4. Pore size distribution of ACFs-BQ obtained by means of the H-K method.

This result implies that some wider pores, close to mesopore, are developed in the fibers. Many investigators [15-19] have been suggested that pores formed by proper activation are generally needle shape and vary in diameter between 1 and 2 nm, but further activation cause surface burn-off resulting in macropore formation. Also, other researchers [20, 21] proposed that the surface oxides of carbon adsorbents formed during activation reduce their sorption capacity caused by the block of pore entrances. Therefore, from the pore size distribution curves of nitrogen adsorption and small hysteresis in Fig. 2, we can understand that there might be some micropores having narrow-necked bottle. Considering the fact that carbon fibers are made up of graphite basal planes in the form of microfibrils with imperfect stacking which form pores or voids, a series of interconnected pore spaces as Everett [22] points out is more likely than discrete bottles.

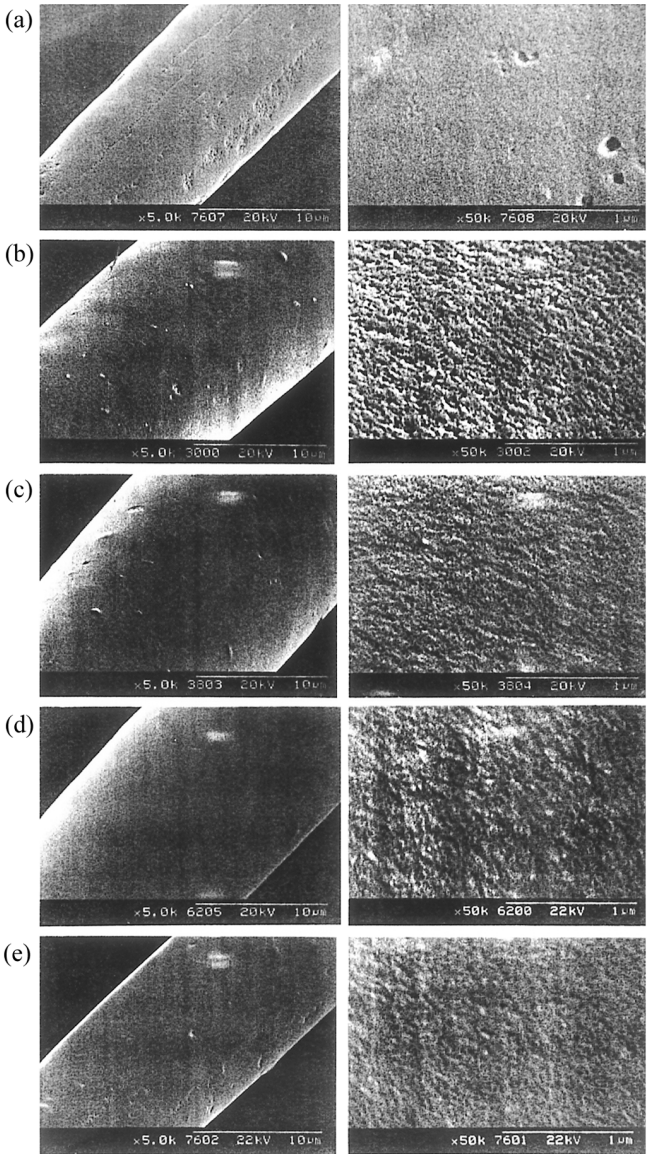

Fig. 5. SEM images of ACF surfaces: (a) 0%, (b) 30%, (c) 38%, (d) 62%, (e) 76% weight loss.

3.2. Surface morphology and properties

Fig. 5 shows the SEM photographs of various burn-off of ACFs-BQ. On the surface of unactivated carbon fiber, there are some coarse pores as expected from the data of specific surface area and average pore diameter. These pores seem to be some ditches along the fiber axis that might be caused by the scratch of nozzle wall. These ditches remained after carbonization and enlarged the specific surface area and average pore diameter of unactivated carbon fiber. The surface of ACF-BQ-30% was also very coarse and quite different from the surface morphology of other ACFs. However, there might be only micropores in the fibers in consideration of large micropore volume and small external surface area. Interestingly, the surface of ACF-BQ becomes smooth with increasing the burn-off. It is believed that the external burn-off removes some larger pores of surface and only micropores develop with the increase of burn-off. The surface morphology of the higher burn-off (62%) shows that there are enormous micropores resulting in high specific surface area of the fibers. However, too much burn-off (76%) makes the surface coarse again. Traces of some ditches remain after high burn-off level.

Surface functional groups of CF-BQ and ACF-BQ were investigated by FT-IR and shown in Fig. 6. A broad absorption band with a maximum at 3450 cm^{-1} seems to arise from vibrations of OH groups of adsorbed water molecules. The spectral range of 1740-1600 cm^{-1} was very important because the functionality of carbon was determined by surface groups existed in this region. The peak around 1700 cm^{-1} was assigned to the carboxyl C=O stretching of non-aromatic carboxylic acid structure [23]. According to previous literature [24], the carboxyl C=O stretching of a carboxylic acid existing in an aromatic ring structure generally appears at 1700-1680 cm^{-1} and its wave number is affected by different peripheral functional groups. Considering the fact that

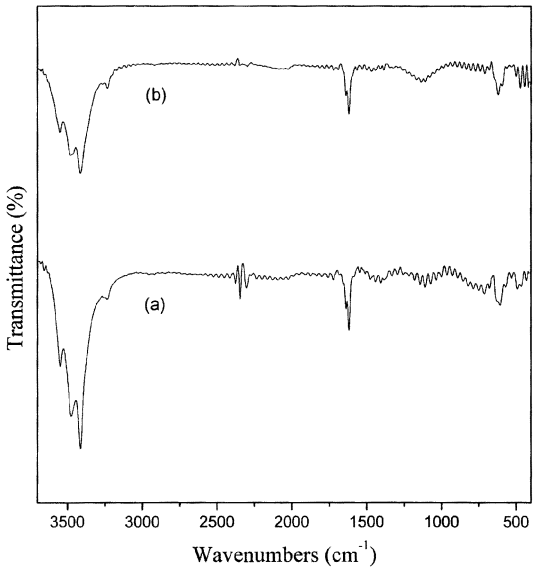

Fig. 6. FT-IR spectra of unactivated and activated carbon fibers: (a) unactivated, (b) 62% weight loss.

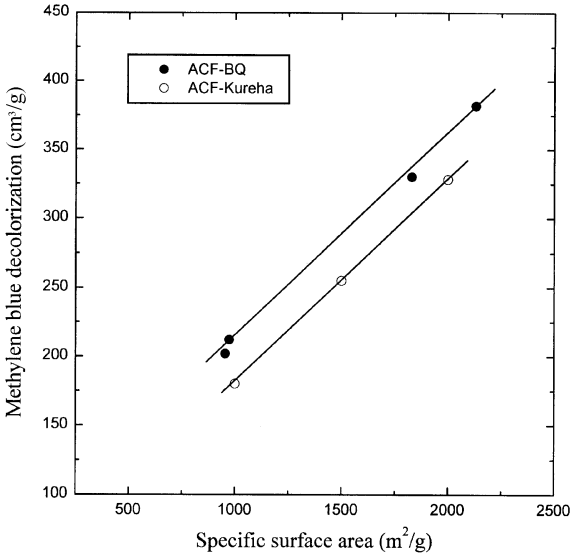

Fig. 7. Methylene blue decolorization capacity of activated carbon fibers.

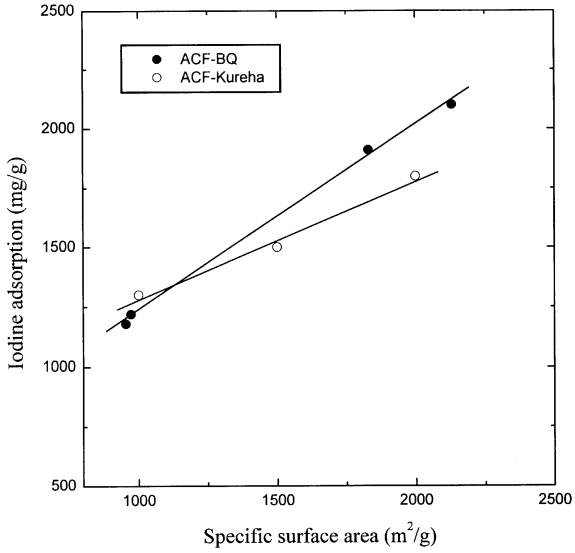

Fig. 8. Iodine adsorption capacity of activated carbon fibers.

the carbonyl peak of the quinone structure appears at 1669 cm^{-1}, the peak at 1667 cm^{-1} could be assigned as a carbonyl peak of conjugated ketone or quinone structure [23-25]. Especially, it was interesting that the broad band at with a maximum at 1140 cm^{-1} was developed as the burn-off of CF-BQ increased. This absorption band can be assigned to C-O and O-H bending/stretching vibration of the phenol group [23-25].

3.3. Adsorption properties

Methylene blue decolorization capacity of ACF-BQ was investigated and shown in Fig. 7. The adsorption of the cationic dye, methylene blue, has been used for a long time for the evaluation of the adsorption properties of active carbons, particularly liquid phase carbons. Moreover, it has been pointed out that when a large molecule, like methylene blue, and smaller, or solvent molecules, like water, are adsorbed on a porous solid the effective surface of adsorbent available to the larger molecule is limited by pore screening or molecular sieving [26, 27]. From the result, the decolorization capacity increased linearly with the increase of specific surface area and is larger than that of ACF-Kureha at the same specific surface area. This fact confirms that the average pore size of ACF-BQ is larger than ACF-Kureha and the ACF-BQ can adsorb larger adsorbate more easily. In addition to that, the surface contained in these pores is presumably all available to methylene blue since this dye molecule has a minimum diameter of about 0.8 nm [28] and the limiting diameter of pores which will admit the molecule has been estimated to be about 1.3 nm [26].

Iodine adsorption capacity of ACF-BQ is shown in Fig. 8. The adsorption capacity increased linearly with the increase of specific surface area as well as methylene blue decolorization. The iodine adsorption capacity of ACF-BQ was higher than that of ACF-Kureha above 1200 m^2/g of specific surface area. This result also indicates that the micropore structure of ACF-BQ is different from ACF-Kureha.

4. Conclusion

The coal tar pitch was chemically modified with 10 wt% BQ and the precursor was melt-spun into pitch fibers, stabilized, carbonized and activated with steam at 900°C.

The weight loss of CF-BQ increased with the increase of activation time but was lower than that of Kureha fiber at the same activation time in spite of larger geometric surface. This means that CF-BQ is thermally more stable than Kureha fiber and the CF-BQ has different orientation structure from other fibers because of oligomeration of precursor pitch.

The nitrogen adsorption isotherms of ACF-BQ show 'Type I' with sharp knee and then plateau. However, there are very thin 'low-pressure hysteresis' on all the isotherms, whose lower closure points are about 0.42-0.45. From the pore size distribution curves of nitrogen, low-pressure hysteresis might be cause by some micropores having narrow-necked bottle; a series of interconnected pore is more likely than discrete bottles.

The micropore volume of unactivated carbon fiber is almost same to the total pore volume, and the external surface area is very small. These micropores must be developed during the carbonization of pitch.

The FT-IR results show that functional groups such as carboxyl, quinone, and phenol were introduced to carbon surface like other isotropic pitch-based ACFs.

Methylene blue decolorization capacity of ACF-BQ increased linearly with the increase of specific surface area. This indicates that the ACF-BQ can adsorb larger adsorbate more easily. Iodine adsorption capacity of ACF-BQ also increased linearly with the increase of specific surface area as well as methylene blue decolorization. The iodine adsorption capacity of ACF-BQ was higher than that of ACF-

Kureha above 1200 m^2/g of specific surface area. This result also shows that the micropore structure of ACF-BQ is different from ACF-Kureha.

References

[1] Donnet, J. B. et al. *Carbon Fibers*, 3rd ed., Marcel Dekker, New York, 1988.
[2] Barr, J. B.; Lewis, I. C. *Carbon* **1978**, *16*, 439.
[3] Mochida, I.; Inaba, T.; Korai, Y.; Fujitsu, H.; Takeshida, K. *Carbon* **1983**, *6*, 543.
[4] Lee, D. J.; Kim, C.; Yang, K. S. in *Extended Abstracts 22th Biennial Conference on Carbon*, American Carbon Society, SanDiego, U.S.A., 1995, 44.
[5] Yang, K. S.; Lee, D. J.; Mochida, I. Extended Abstracts 23th Annual Meeting of the Carbon Society of Japan, Nagasaki, Japan, 1996, 86.
[6] Rodriguez-Reinoso, F.; Martin-Martinez, J. M.; Prado-Burguete, C.; McEnaney, B. *J. Phys. Chem.* **1987**, *91*, 515.
[7] Shin, S.; Yoon, S. H.; Mochida, I. *Carbon* **1997**, *35*, 1739.
[8] Ryu, S. K.; Rhee, B. S.; Pusset, N.; Ehrburger, P. Extended Abstracts, Carbon 90, Paris, France, 1990, 96.
[9] Ryu, S. K. *High Temp.-High Press.* **1990**, *22*, 345.
[10] Harris, M. R. *Chem. Ind.* **1965**, 269.
[11] Gregg, S. J.; Langford, J. F. *J. Chem. Soc. Faraday Trans. I.* **1977**, *73*, 747.
[12] Avery, R. G.; Ramsay, J. D. F. *J. Colloid Interface Sci.* **1973**, *42*, 597.
[13] Tayyab, M. M.; Ph. D. Thesis, Brunel University, 1971.
[14] Kaneko, K.; Setoyama, N.; Suzuki, T. *Characterization of Porous Solids III, Studies in Surface and Catalysis*, vol. 87, Elsevier Science, B. V., 1994; p 593.
[15] Perret, R.; Ruland, W. *J. Appl. Crystallog.* **1970**, *3*, 525.
[16] Fourdeux, A.; Perret, R.; Ruland, W. *Carbon Fibers-Their Composites and Applications*, The Plastics Institute, London, 1971, 57.
[17] Johnson, D. J.; Tyson, C. N. *Br. J. Appl. Phys.* **1969**, *D3*, 526.
[18] Donnet, J. B.; Ehrburger, P. *Carbon* **1973**, *15*, 143.
[19] Bacon, R.; Silvaggi, A. F. *Carbon* **1971**, *9*, 321.
[20] Billinge, B. H. M.; Evans, M. G. *J. Chim, Phys.* **1984**, *82*, 779.
[21] Barton, S. S.; Koresh, J. E. *Carbon* **1984**, *22*, 481.
[22] Everett, D. H. *The Solid-Gas Interface*, Dekker, New York, vol. 2, 1967, p 1055.
[23] Colthup, N. B.; Day, L.; Wilberley, S. *Introduction to Infrared and Raman Spectroscopy,* Academic Press, London, 1975.
[24] Pretsch, Clerc, Seibl, and Simon, *Tables of Spectral Data for Structure Determination of Organic Compounds*, 2nd ed., Springer-Verlag, New York, 1989.
[25] Fanning, P. E.; Vannice, M. A. *Carbon* **1993**, *31*, 721.
[26] Graham, D. *J. Phys. Chem.* **1955**, *59*, 896.
[27] Dubinin, M. M.; Zaverina, E. D. *Acta. Phys. Chim. U.S.S.R.* **1936**, *4*, 647.
[28] Kipling, J. J.; Wilson, R. D. *J. Appl. Chem.* **1960**, *10*, 109.